

# CHALMERS



## Aeration Control of Activated Sludge Basins

*Master's Thesis in Automatic Control*

ANDREAS SANDBERG

Department of Signals & Systems  
Systems, Control & Mechatronics  
CHALMERS UNIVERSITY OF TECHNOLOGY  
Gothenburg, Sweden 2016  
Master's Thesis EX100/2016



## **Abstract**

The aeration of activated sludge basins is expensive. In this thesis, a model of the activated sludge basins at Gryaab's wastewater treatment plant, Ryaverket in Gothenburg, Sweden, is created for the purpose of simulating different control strategies. The main effluent pollutant investigated are nitrate and nitrite, NO, and biological oxygen demand, BOD. Optimizations are performed to find better control strategies for the aeration than the currently used strategy. Results show that there is a large potential in reducing both costs and effluent concentrations through simple change of operations. The recommended new control strategy suggested is to aerate 60 % with set points below half the currently used set points.



## **Acknowledgements**

I would like to thank my supervisor Torsten Wik for his help with this thesis, Nanette for her patience and Viktor and Julia for the motivation.

Andreas Sandberg, Gothenburg 2016-11-18



# Contents

<b>1</b>	<b>Introduction</b>	<b>1</b>
<b>2</b>	<b>The Plant</b>	<b>3</b>
2.1	Description . . . . .	3
2.1.1	Activated sludge basins . . . . .	4
2.1.2	Nitrification and denitrification . . . . .	4
2.2	Plant model . . . . .	5
2.2.1	Mantis . . . . .	5
2.2.2	Simulink . . . . .	9
2.2.3	The influent . . . . .	10
2.2.4	The effluent . . . . .	14
<b>3</b>	<b>Control strategy</b>	<b>15</b>
3.1	Lambda tuning . . . . .	15
3.2	Optimal airflow . . . . .	16
3.3	Same airflow . . . . .	17
<b>4</b>	<b>Simulation</b>	<b>19</b>
4.1	Finding the optimal airflow . . . . .	19
4.2	The current setup . . . . .	20
4.2.1	Lambda tuning . . . . .	20
4.3	Same airflow across all tanks . . . . .	21
4.4	Minimum <i>BOD</i> , same total airflow as current . . . . .	22
4.5	Minimum <i>NO</i> , same total airflow as current . . . . .	22
4.6	Minimum total airflow, same <i>BOD</i> as current . . . . .	22
4.7	Minimum total airflow, same <i>NO</i> as current . . . . .	23
4.8	Simulations using variable influent . . . . .	23
<b>5</b>	<b>Results</b>	<b>25</b>
5.1	The current setup . . . . .	25

5.2	Same airflow across all tanks . . . . .	25
5.3	Minimum <i>BOD</i> , same total airflow as current . . . . .	25
5.4	Minimum <i>NO</i> , same total airflow as current . . . . .	27
5.5	Minimum total airflow, same <i>BOD</i> as current . . . . .	27
5.6	Minimum total airflow, same <i>NO</i> as current . . . . .	28
5.7	Simulations using variable influent . . . . .	29
<b>6</b>	<b>Discussion</b>	<b>31</b>
<b>7</b>	<b>Conclusion</b>	<b>33</b>
<b>A</b>	<b>Tables</b>	<b>35</b>
	<b>Bibliography</b>	<b>38</b>



# 1

## Introduction

Wastewater treatment plants (WWTP) has more and harder regulations on their effluent today than ever before. Two of these regulations concern the concentration of nitrogen and biochemical oxygen demand (*BOD*). The consequence of the regulation on nitrogen can, in this work, be translated to reduction demands on nitrate and nitrite (*NO*). By adding an external carbon source to the wastewater more *NO* can be removed, this is expensive and less carbon added is therefore preferred. To remove as much biodegradable hydrocarbons (*BOD*) as possible, the wastewater is aerated. This, however, is also expensive and therefore a strategy for controlling this aeration is studied in this thesis. *BOD* can be used as carbon source for the removal of *NO* if there is no oxygen in the wastewater. The capacity to remove *NO* is higher when a smaller volume of the basin is aerated. On the other hand *BOD* is better removed by aerating a larger part of the basins. A control strategy that aerates the basins in a more cost effective way is investigated. The plant studied in this work is Gryaab's plant Ryaverket in Göteborg, Sweden.



# 2

## The Plant

### 2.1 Description

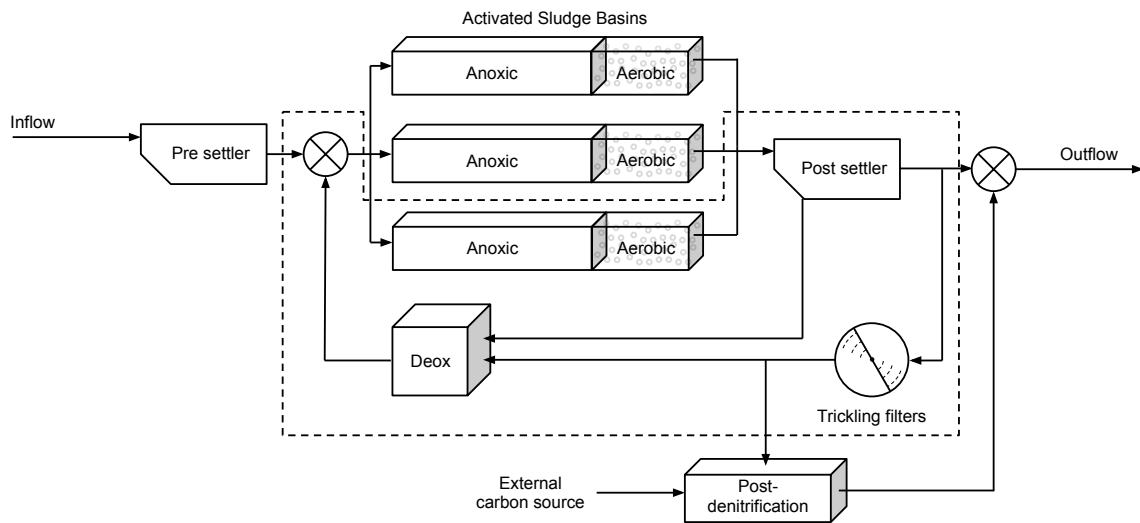


**Figure 2.1:** The plant investigated.

The wastewater treatment at Ryaverket, which is illustrated in Figure 2.1, is roughly divided into three parts; mechanical, biological and chemical. The mechanical part applies filtering in the beginning of the process which removes trash and paper, and finer filters are also used at the end of the process where small particles are removed. In the chemical part of the process, iron sulfate is added to the wastewater to obtain a precipitation of phosphorus that can be removed through sedimentation.

In the biological part, bacteria decomposes organic materials and releases the nutrient

nitrogen from the wastewater. Ryaverket has three parallel lines of activated sludge basins. In the basins, bacteria decomposes organic matter in two different parts. In the first part of the basins, the anoxic part, no air is added, and when oxygen is lacking nitrate and nitrite is used in the degradation, which has the effect that they are converted into nitrogen gas. In the second part, the aerobic part, the basin is aerated and the bacteria uses oxygen instead to decompose the organic matter.

After the activated sludge basins, the wastewater is sedimented to remove the sludge. About half of the settled wastewater is sent to the last filtering process before it leaves the plant, and the other half goes through trickling filters where ammonium is nitrified. One part of the nitrified wastewater goes to basins for post denitrification, where a carbon source is added to remove the remaining nitrate. The rest of the flow, along with some of the sludge from the sedimentation, is deoxidized and mixed with the influent to the activated sludge basins [1].

### 2.1.1 Activated sludge basins

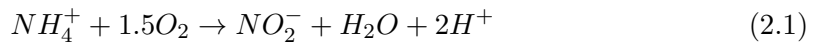
The three parallel lines of activated sludge basins have the same layout. The first 40 % of the basins is not aerated, the last 40 % is always aerated and the 20 % in the middle of the basins can be either aerated or not aerated.

In the basins, heterotrophic bacteria grows by using oxygen and organic carbon to make biomass and energy.

The bacteria behave differently if there is oxygen present (aerobic), nitrate present (anoxic) or neither oxygen nor nitrate present (anaerobic). When the wastewater is aerobic the bacteria prefer to use oxygen rather than nitrate, but if the conditions are anoxic the bacteria grow utilizing the oxygen in the nitrite and nitrate. When neither oxygen nor nitrate or nitrite is present the growth of the bacteria is stalled [2].

### 2.1.2 Nitrification and denitrification

The conversion of ammonia into nitrate is a two step procedure. Both steps are done by autotrophic bacteria but of different species. The first step, to oxidize ammonia into nitrite, is

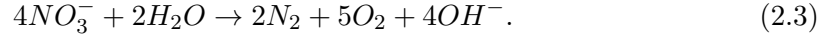


and the second step that convert nitrite into nitrate is



These two steps are mainly taking place in the trickling filters after the activated sludge basins. Then some of the nitrified wastewater is mixed with the influent to the activated sludge basins, and some goes through the post-denitrification basins. In the post-denitrification basins, a source of carbon has to be added because the easily biodegradable compounds needed there have been removed earlier in the process.

Denitrification is when nitrate is transformed into nitrogen gas. This occurs when the conditions are anoxic and the heterotrophic bacteria use nitrate instead of oxygen to decompose the biodegradable compounds giving an approximate stoichiometry for nitrogen



This is done in the anoxic part of the activated sludge basins [3]. Note that all stoichiometric expressions presented are simplified and only contains the components relevant here.

## 2.2 Plant model

To be able to simulate different control strategies for the aeration and get a deeper understanding of the process, a model of the activated sludge basins was developed in Simulink/Matlab.

The model is limited to the activated sludge basins, the deox basins, the post-settler and the trickling filters, as illustrated inside the dashed line in Figure 2.1.

A lithium trace study has shown that each of the three lines can be modelled as eight perfectly mixed tanks connected in series, as shown in Figure 2.2 [4].

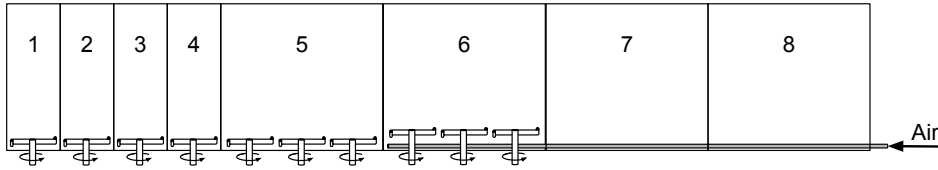


**Figure 2.2:** Tanks 1-5 are stirred but not aerated (anoxic), tank 6 is stirred and can be aerated and tanks 7-8 are not stirred and always aerated (aerobic).

The activated sludge basins is one of many parts of the wastewater treatment plant. As can be seen in Figure 2.1, there are more processes included in the same loop as the wastewater that passes through the basins. To achieve a complete feedback loop the trickling filters and secondary sedimentation are implemented as ideal components, that is, all ammonia is converted to nitrate in the trickling filters, as in equations (2.1) and (2.2), and all particles are removed in the post-settler.

### 2.2.1 Mantis

To describe the chemical processes in the activated sludge process a mathematical model is used.

In a project called Morya 2010, the complete plant at Ryaverket was modelled in an application called GPS-X from Hydromantis, Inc. The mathematical model used in GPS-X is called Mantis and is a further development of the Activated Sludge Model No.

**Table 2.1:** Arrhenius coefficients  
for the kinetic parameters.

$\theta_{\mu_H}$	1.050
$\theta_{\mu_A}$	1.123
$\theta_{k_H}$	1.072
$\theta_{k_A}$	1.029
$\theta_{b_H}$	1.029
$\theta_{b_A}$	1.072

1 (ASM1)[4] [2].

Mantis and ASM1 are identical except for three improvements in the Mantis model:

1. Additional growth processes are introduced for the autotrophic and the heterotrophic organisms. The organisms can use nitrate as a nutrient source under conditions of low ammonia and high nitrate.
2. The kinetic parameters are temperature dependent. An Arrhenius equation is used to describe the temperature dependence of some of the kinetic parameters. For the maximum specific growth rate of heterotrophs,  $\mu_H$ , the equation is

$$\mu_H = \mu_{H,20^\circ\text{C}} \cdot \theta_{\mu_H}^{(T-20^\circ\text{C})}, \quad (2.4)$$

where  $\mu_{H,20^\circ\text{C}}$  is  $\mu_H$  at  $20^\circ\text{C}$ ,  $\theta_{\mu_H}$  is the temperature coefficient for  $\mu_H$ , and  $T$  is the temperature. The Arrhenius coefficients used in the model are listed in Table 2.1.

3. Denitrification in aerobic processes.

Mantis is described by the Petersen matrix in Table 2.2. The matrix contains fourteen components and ten processes.

Table 2.2: Petersen matrix for Mantis

Component		$i$	1	2	3	4	5	6	7	8	9	10	11	12	13	14	Process rate, $\rho_j$
$j$	$S_f$	$S_S$	$X_f$	$X_S$	$X_{BH}$	$X_{BA}$	$X_U$	$X_{ND}$	$S_O$	$S_{NO}$	$S_{NN}$	$S_{NH}$	$S_{ND}$	$S_{ALK}$			
1	Aerobic growth of heterotrophs on $S$ as with $u_{ph}$	$\frac{-1}{Y_H}$			1				$-\frac{(1-Y_H)}{Y_H}$						$-\frac{ubn}{14}$	$\mu_H \left( \frac{S_S}{K_{SH}+S_S} \right) \left( \frac{S_O}{K_{OH}+S_O} \right) \left( \frac{S_{NH}}{K_{NH}+S_{NH}} \right) \left( \frac{S_{ALK}}{K_{ALK}+S_{ALK}} \right) X_{BH}$	
2	Anoxic growth of heterotrophs on $S$ as with $u_{ph}$	$\frac{-1}{Y_H}$			1				$-\frac{(1-Y_H)}{2.86Y_H}$						$-\frac{ubn}{14}$	$\eta_g \cdot \mu_H \left( \frac{S_S}{K_{SH}+S_S} \right) \left( \frac{K_{AD}}{K_{AD}+S_O} \right) \left( \frac{S_{NH}}{K_{NH}+S_{NH}} \right) \left( \frac{S_{NO}}{K_{NO}+S_{NO}} \right) \left( \frac{S_{ALK}}{K_{ALK}+S_{ALK}} \right) X_{BH}$	
3	Aerobic growth of heterotrophs on $S$ as with $u_{ph}$	$\frac{-1}{Y_H}$			1				$-\frac{(1-Y_H)}{Y_H}$						$-\frac{ubn}{14}$	$\mu_H \left( \frac{S_S}{K_{SH}+S_S} \right) \left( \frac{S_O}{K_{OH}+S_O} \right) \left( \frac{K_{NH}}{K_{NH}+S_{NH}} \right) \left( \frac{S_{NO}}{K_{NO}+S_{NO}} \right) \left( \frac{S_{ALK}}{K_{ALK}+S_{ALK}} \right) X_{BH}$	
4	Anoxic growth of heterotrophs on $S$ as with $u_{ph}$	$\frac{-1}{Y_H}$			1				$-\frac{(1-Y_H)}{2.86Y_H}$						$-\frac{ubn}{14}$	$\eta_g \cdot \mu_H \left( \frac{S_S}{K_{SH}+S_S} \right) \left( \frac{K_{AD}}{K_{AD}+S_O} \right) \left( \frac{K_{NH}}{K_{NH}+S_{NH}} \right) \left( \frac{S_{NO}}{K_{NO}+S_{NO}} \right) \left( \frac{S_{ALK}}{K_{ALK}+S_{ALK}} \right) X_{BH}$	
5	Hydrolysis of heterotrophic entrapped organic nitrogen				$1 - f_{uh}$		$f_{uh}$	$\frac{ubn}{-f_{uh} \cdot ubn}$								$b_H \cdot X_{BH}$	
6	Hydrolysis of organic nitrogen	1			$-1$											$k_H \left( \frac{X_S/X_{NH}}{K_{X+S}/X_{BH}} \right) \left( \left( \frac{S_O}{K_{OH}+S_O} \right) + \eta_h \left( \frac{K_{OH}}{K_{OH}+S_O} \right) \left( \frac{S_{NO}}{K_{NO}+S_{NO}} \right) \right) X_{BH}$	
7	Ammonification of soluble organic nitrogen							$-1$								$r_0 \cdot \left( \frac{X_{ND}}{X_S} \right)$	
8	Growth of autotrophs								$-\frac{(4.67-Y_A)}{Y_A}$							$k_A \cdot S_{ND} \cdot X_{BH}$	
9	Decay of autotrophs				$1 - f_{ua}$					$\frac{Y_A}{Y_A}$						$\mu_A \left( \frac{S_{NH}}{K_{NA}+S_{NH}} \right) \left( \frac{S_{NH}}{K_{NA}+S_{NH}} \right) \left( \frac{S_O}{K_{OA}+S_O} \right) \left( \frac{S_{ALK}}{K_{AKA}+S_{ALK}} \right) X_{BA}$	
10					$-1$	$f_{ua}$	$-f_{ua} \cdot ubn$									$b_0 \cdot X_{BA}$	
Soluble inert organics ( $gCODm^{-3}$ )																	
Readily biodegradable soluble substrate ( $gCODm^{-3}$ )																	
Particulate inert organics ( $gCODm^{-3}$ )																	
Slowly biodegradable particulate substrate ( $gCODm^{-3}$ )																	
Active heterotrophic biomass ( $gCODm^{-3}$ )																	
Active autotrophic biomass ( $gCODm^{-3}$ )																	
Unbiodegradable particulates from cell decay ( $gCODm^{-3}$ )																	
Particulate biodegradable organic nitrogen ( $gNm^{-3}$ )																	
Oxygen ( $g(-COD)m^{-3}$ )																	
Nitrate and nitrite nitrogen ( $gNm^{-3}$ )																	
Dinitrogen ( $gNm^{-3}$ )																	
Ammonia nitrogen ( $gNm^{-3}$ )																	
Soluble biodegradable organic nitrogen ( $gNm^{-3}$ )																	
Alkalinity ( $molem^{-3}$ )																	

The mass balance for a specific component within a system is

$$Accumulation = Inflow - Outflow + Reaction, \quad (2.5)$$

where the reaction rate,  $r$ , for a component,  $i$ , is obtained by summing the products of the coefficients  $\nu_{ij}$  and the process rates  $\rho_j$  over  $j$ , i.e.

$$r_i = \sum_j \nu_{ij} \rho_j. \quad (2.6)$$

For example, the reaction rate for active autotrophic biomass,  $X_{BA}$ , is

$$r_{X_{BA}} = \mu_A \left( \frac{S_{NH}}{K_{NH} + S_{NH}} \right) \left( \frac{S_{NH}}{K_{NA} + S_{NH}} \right) \left( \frac{S_O}{K_{OA} + S_O} \right) \left( \frac{S_{ALK}}{K_{ALK} + S_{ALK}} \right) X_{BA} - b_a \cdot X_{BA}. \quad (2.7)$$

In a perfectly mixed tank the dynamic behaviour of the active autotrophic biomass becomes

$$V \cdot \frac{dX_{BA}}{dt} = Q \cdot (X_{BA,In} - X_{BA}) + V \cdot r_{X_{BA}}, \quad (2.8)$$

where  $V$  is the tank volume,  $Q$  is the flow through the tank and  $X_{BA,In}$  is the incoming concentration of the biomass. By applying (2.8) to each component in the Petersen matrix and every tank, a model of the complete activated sludge process is achieved.

Since some of the tanks are aerated an additional term is added to the dynamic behaviour of dissolved oxygen,  $S_O$ . The oxygen that is transferred from the air bubbles into the water is determined by

$$V \cdot K_L \cdot a \cdot (S_{O,Sat} - S_O), \quad (2.9)$$

where  $K_L$  is the transfer coefficient for oxygen into the water,  $a$  is the ratio of bubble area to water volume,  $S_{O,Sat}$  is the saturation concentration for the dissolved oxygen and  $S_O$  is the dissolved oxygen concentration. Here,  $S_{O,Sat}$  is temperature dependent as given by Wik [5] as

$$S_{O,Sat} = 14.53 - 0.411T + 9.6 \cdot 10^{-3}T^2 - 1.2 \cdot 10^{-4}T^3 \text{ gO}_2/\text{m}^3. \quad (2.10)$$

The transfer coefficient for oxygen into the water,  $K_L a$ , is described by

$$K_L a = k_1(1 - e^{-k_2 \cdot q_{O_2}}), \quad (2.11)$$

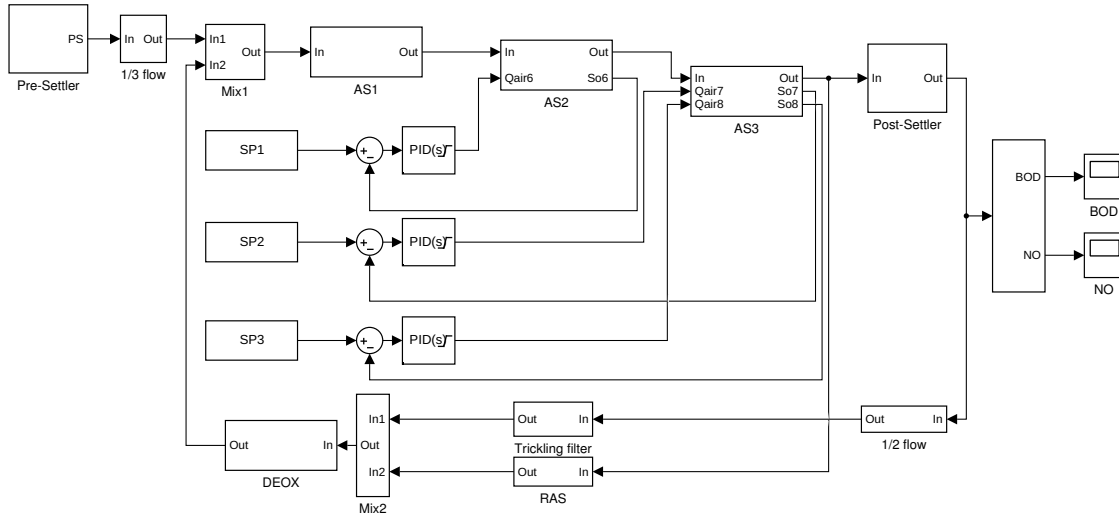
where  $q_{O_2}$  is the airflow and  $k_1$  and  $k_2$  have been estimated for Ryaverket to the values in Table 2.3 by Hedegård and Wik [6].



**Table 2.3:** Estimated parameters for  $K_L a$ .

	Tank 6	Tank 7	Tank 8
$k_1$	391	326	163
$k_2$	$1.58 \cdot 10^{-4}$	$1.90 \cdot 10^{-4}$	$3.80 \cdot 10^{-4}$

### 2.2.2 Simulink

**Figure 2.3:** Simulink model

The model of Ryaverket was implemented in Simulink (see Figure 2.3). The influent to the model is the wastewater that comes from the pre-settler. To represent the wastewater, the components in the Petersen matrix as well as the temperature and flow rate are used as variables passed between the blocks. The influent is mixed with the recirculated wastewater from the deox tanks. Then the wastewater goes through the activated sludge basins and further to the post-settler. Half of the settled wastewater is transported to the effluent and the other half passes the trickling filters. After the trickling filters one part of the wastewater goes to the post-denitrification and the other part gets mixed

with the recycled sludge from the post-settler into the deox tanks.

The Mantis model was written as a C-file and implemented as a system-function (S-function) in Simulink. One S-function block represents one perfectly mixed tank in the activated sludge basin as seen in Figure 2.2. As state variables and input/output to the S-function the components in the Petersen matrix in Table 2.2, the flow rate, airflow rate and the temperature are used. The states of the S-function are the components in the Petersen matrix, and the change in each component is calculated using the process rate and coefficients as in Equations 2.7 and 2.8.

The three parts of the activated sludge basins, i.e. anoxic, mixed and aerobic, are in the blocks AS1, AS2 and AS3 in Figure 2.3. The aerobic part is shown in Figure 2.4.

Tanks 1-4, in Figure 2.2, are implemented in AS1, tanks 5 and 6 in AS2 and tanks 7 and 8 in AS3.

The deoxidation tanks is modelled as ten reaction tanks connected in series. These tanks effectively removes all  $S_O$  from the wastewater.

A very simple model of the trickling filters is used. The model simply converts all ammonia nitrogen ( $S_{NH}$ ) to nitrate and nitrite nitrogen ( $S_{NO}$ ).

The post-settler is also modelled as ideal, removing all suspended solids.

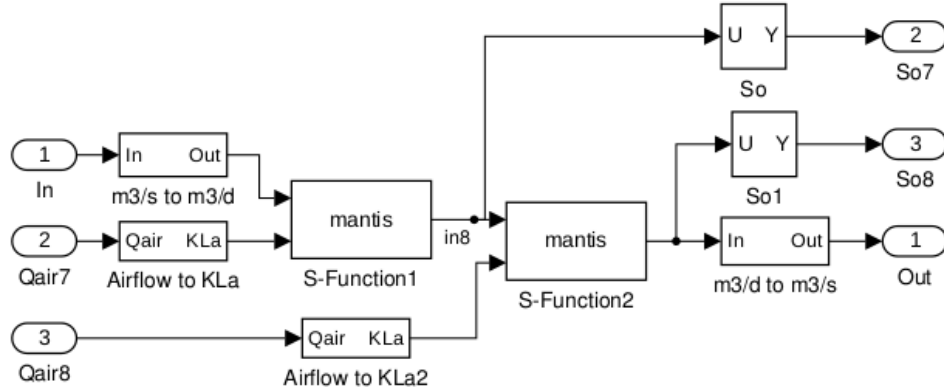


**Figure 2.4:** Simulink model of two aerated tanks (AS3).

The components used in the model are listed in Table 2.4, the composite variables in Table 2.5, the stoichiometric parameters in Table 2.6 and the kinetic parameters in Table 2.7. All values for the different parameters are from the Morya 2010 project [4].

To verify the model, simulations were executed with identical inputs as the GPS-X model used in the Morya 2010 project. The output, were nearly identical.

### 2.2.3 The influent

A two month summer period measurement series from Ryaverket are used as input to the simulations. Temperature ( $Temp$ ), flow ( $Q$ ), chemical oxygen demand ( $COD$ ),  $S_{NH}$  and  $S_{NO}$  are considered as measured in the simulations. All these variables used in

**Table 2.4:** Components

Inorganic Suspended Solids		
$X_{II}$	inert inorganic suspended solids	$g/m^3$
Organic Variables		
$S_I$	soluble inert organic material	$gCOD/m^3$
$S_S$	readily biodegradable substrate	$gCOD/m^3$
$X_I$	particulate inert organic material	$gCOD/m^3$
$X_S$	slowly biodegradable substrate	$gCOD/m^3$
$X_{BH}$	active heterotrophic biomass	$gCOD/m^3$
$X_{BA}$	active autotrophic biomass	$gCOD/m^3$
$X_U$	unbiodegradable particulate matter from cell decay	$gCOD/m^3$
Dissolved Oxygen		
$S_O$	dissolved oxygen	$gO_2/m^3$
Nitrogen compounds		
$S_{NH}$	free and ionized ammonia	$gN/m^3$
$S_{ND}$	soluble biodegradable organic nitrogen	$gN/m^3$
$X_{ND}$	particulate biodegradable organic nitrogen	$gN/m^3$
$S_{NO}$	nitrate and nitrite nitrogen	$gN/m^3$
$S_{NN}$	dissolved dinitrogen	$gN/m^3$
Alkalinity		
$S_{ALK}$	alkalinity	$mole/m^3$

Mantis are not measured directly. By using *COD* fractions in the same way that is used in the Morya 2010 project [4] the measured *COD* is divided into the different variables.

Most of the data are daily averages and since the aeration process has a time response in less than a day a variation is added. Therefore, the variation from a set of test data taken from the COST simulation benchmark described by Copp [7], was scaled to have the same daily average as the collected measurement series, i.e.

$$\tilde{S}_S(t) = \hat{S}_S(t) + \hat{S}_S(t) \cdot \frac{COST_{S_S}(T) - \frac{1}{N} \sum_{i=0}^N (COST_{S_S}(i))}{\frac{1}{N} \sum_{i=0}^N (COST_{S_S}(i))}, \quad (2.12)$$

where  $\tilde{S}_S(t)$  is the measured mean value with added variations at time  $t$ ,  $\hat{S}_S(t)$  is the measured mean value at time  $t$ ,  $COST_{S_S}(T)$  is a value from the COST data series at

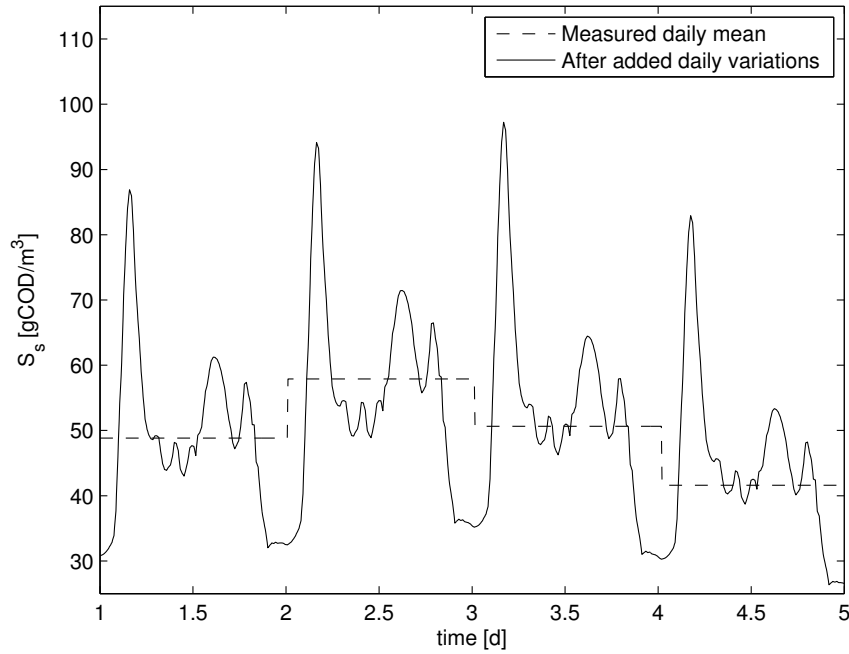
**Table 2.5:** Composite variables

Organic Matter ( $COD$ , $BOD$ , $TSS$ )		
$S_{COD}$	filtered $COD$	$gCOD/m^3$
$X_{COD}$	particulate $COD$	$gCOD/m^3$
$COD$	total $COD$	$gCOD/m^3$
$S_{BOD}$	filtered carbonaceous $BOD_5$	$gO_2/m^3$
$X_{BOD}$	particulate carbonaceous $BOD_5$	$gO_2/m^3$
$BOD$	total carbonaceous $BOD_5$	$gO_2/m^3$
$S_{BOD_U}$	filtered ultimate carbonaceous $BOD$	$gO_2/m^3$
$X_{BOD_U}$	particulate ultimate carbonaceous $BOD$	$gO_2/m^3$
$BOD_U$	total ultimate carbonaceous $BOD$	$gO_2/m^3$
$VSS$	volatile suspended solids	$g/m^3$
$X$	total suspended solids	$g/m^3$
Inorganic Matter		
$X_{ISS}$	inert inorganic suspended solids	$g/m^3$
Nitrogen compounds		
$S_{TKN}$	filtered $TKN$	$gN/m^3$
$X_{TKN}$	particulate $TKN$	$gN/m^3$
$TKN$	total $TKN$	$gN/m^3$
$TN$	total nitrogen	$gN/m^3$

the  $T$ 'th part of a day divided in  $N$  parts. The daily mean measurements are linearly interpolated to get data points between each daily measurement. The result for the component of readily biodegradable soluble substrate ( $S_S$ ) is shown in Figure 2.5, where we can note that the daily variations are the same from one day to another.

**Table 2.6:** Stoichiometric parameters at 20 °C

Composite Variable Stoichiometry		
Organic Fractions		
$i_{CV}$	$XCOD/VSS$	1.480 $gCOD/gVSS$
$f_{BOD}$	$BOD_5/BOD_U$ ratio	0.660 -
Nutrient Fractions		
$i_{bhn}$	N content of active biomass	0.068 $gN/gCOD$
$i_{uhn}$	N content of endogenous/inert mass	0.068 $gN/gCOD$
Model Stoichiometry		
Active Heterotrophic Biomass		
$Y_H$	heterotrophic yield	0.666 $gCOD/gCOD$
$f_{UH}$	heterotrophic endogenous fraction	0.080 $gCOD/gCOD$
Active Autotrophic Biomass		
$Y_A$	autotrophic yield	0.240 $gCOD/gN$
$f_{UA}$	autotrophic endogenous fraction	0.080 $gCOD/gCOD$

**Figure 2.5:** The measured daily mean of readily biodegradable soluble substrate ( $S_s$ ) and the same variable with daily variation from Copp [7].

**Table 2.7:** Kinetic parameters at 20 °C

Active Heterotrophic Biomass		
$\mu_H$	heterotrophic maximum specific growth rate	3.20 1/d
$K_{SH}$	readily biodegradable substrate half saturation coefficient	5.00 gCOD/m <sup>3</sup>
$K_{OH}$	aerobic oxygen half saturation coefficient	0.20 gO <sub>2</sub> /m <sup>3</sup>
$K_{AD}$	anoxic oxygen half saturation coefficient	0.20 gO <sub>2</sub> /m <sup>3</sup>
$\eta_g$	anoxic growth factor	0.50 -
$K_{NO}$	nitrate half saturation coefficient	0.10 gN/m <sup>3</sup>
$K_{NH}$	ammonia (as nutrient) half saturation coefficient	0.05 gN/m <sup>3</sup>
$b_H$	heterotrophic decay rate	0.62 1/d
$K_{ALK}$	alkalinity half saturation coefficient	0.10 mole/m <sup>3</sup>
Active Autotrophic Biomass		
$\mu_A$	autotrophic maximum specific growth rate	0.90 1/d
$K_{NA}$	ammonia (as substrate) half saturation coefficient	0.70 gN/m <sup>3</sup>
$K_{OA}$	oxygen half saturation coefficient	0.25 gO <sub>2</sub> /m <sup>3</sup>
$b_A$	autotrophic decay rate	0.17 1/d
$K_{ALKA}$	alkalinity half saturation coefficient for autotrophic growth	0.50 mole/m <sup>3</sup>
Hydrolysis		
$K_h$	maximum specific hydrolysis rate	3.00 1/d
$K_X$	slowly biodegradable substrate half saturation coefficient	0.10 gCOD/gCOD
$\eta_h$	anoxic hydrolysis factor	0.60 -
Ammonification		
$K_a$	ammonification rate	0.08 m <sup>3</sup> /gCOD/d

In simulations used for optimization a constant input is required to keep the number of variables at a minimum. In these scenarios a mean value of the whole dry summer period is used.

#### 2.2.4 The effluent

The parts of the effluent that are affected by aeration and regulated by restrictions is total nitrogen (*TKN*) and biochemical oxygen demand (*BOD*). Both have an upper limit for the yearly average of 10 mg/l [8].

# 3

## Control strategy

The carbon source is a cost that should be minimized. Therefore it is preferred that as much as possible of the nitrate is removed in the activated sludge basins rather than in the post-denitrification basins.

The control currently in use at Ryaverket are PI controllers that keep the dissolved oxygen at a given set point, usually 2 mg/l [4]. Only the last 40 % of the activated sludge basins are aerated. The concentration of dissolved oxygen is continually measured in tank 6, 7 and 8. These measured values are used as feedback signals to the PI controllers, having the set point value as input and the airflow into the basins as controller output.

If the dissolved oxygen ( $S_O$ ) is too low, unwanted bacteria has a tendency to increase and disturb the post-settler because of poor settling properties. Usually this is prevented by keeping the dissolved oxygen above 2 mg/l in the last tank [9]. However, a study at Ryaverket showed no significant change in the quality of the effluent after a short period with an oxygen concentration of 1 mg/l [10].

### 3.1 Lambda tuning

To tune the PI-controller in this study the Lambda method is used, which is a method widely used in the process industry to tune PI controllers [11].

The part of the tank that is aerated using a PI controller is approximated as a first order process described by

$$G(s) = K_p \frac{e^{-sL}}{1 + sT}, \quad (3.1)$$

where  $K_p$  is the static gain,  $L$  is the dead time and  $T$  is the time constant of the process  $G(s)$ . These parameters are approximated by a step response.

A PI controller has the transfer function

$$G_c(s) = K_c \frac{1 + sT_i}{sT_i} \quad (3.2)$$

where  $K_c$  is the controller gain and  $T_i$  is the integral time. The closed loop transfer function is specified as

$$G_{cl}(s) = \frac{e^{-sL}}{1 + sT_{cl}} \quad (3.3)$$

where  $T_{cl}$  is the time constant of the closed loop.

Using (3.2) to control (3.1) the closed loop system can be written as

$$G_{cl}(s) = \frac{GG_c}{1 + GG_c} = \frac{K_c K_p (1 + sT_i) e^{-sL}}{(1 + sT) sT_i + K_p K_c (1 + sT_i) e^{-sL}} \quad (3.4)$$

Choosing  $T_i = T$  in (3.4) to cancel the pole at  $1/T$  gives

$$G_{cl}(s) = \frac{K_c K_p e^{-sL}}{sT + K_p K_c e^{-sL}} = \frac{e^{-sL}}{\frac{sT}{K_p K_c} + e^{-sL}} \quad (3.5)$$

Using  $1 - sL$  as an approximation for  $e^{-sL}$  in the denominator of (3.5) we get

$$G_{cl}(s) = \frac{e^{-sL}}{1 + s \left( \frac{T}{K_p K_c} - L \right)} \quad (3.6)$$

By comparing (3.3) with (3.6) we get

$$K_c = \frac{T}{K_p(T_{cl} + L)} \quad (3.7)$$

$$T_i = T \quad (3.8)$$

The desired time constant for the closed loop system,  $T_{cl}$ , is related to the process using

$$T_{cl} = \lambda T \quad (3.9)$$

if  $T > L$  and

$$T_{cl} = \lambda L \quad (3.10)$$

if  $L > T$ , where  $\lambda$  usually is chosen between 0.5 and 3.0. A smaller  $\lambda$  results in a fast response and a larger  $\lambda$  gives a slow system that is less sensitive to parameter variations.

## 3.2 Optimal airflow

The criteria to minimize the aeration cost is, according to the staff at Ryaverket, approximately the same as minimizing the total airflow into the activated sludge basins.



By choosing the current values,  $BOD_{current}$  and  $NO_{current}$ , as maximal values allowed in the optimizations, no impairment is possible. The problem is described by

$$\begin{aligned}
 &\text{minimize} && q_{O_2,6} + q_{O_2,7} + q_{O_2,8} \\
 &\text{subject to} && BOD \leq BOD_{current} \\
 & && NO \leq NO_{current} \\
 & && q_{O_2,X} \leq q_{O_2,X,max} \quad X \in [6,7,8] \\
 & && S_{O,8} \geq 1
 \end{aligned} \tag{3.11}$$

where  $q_{O_2,6}$ ,  $q_{O_2,7}$  and  $q_{O_2,8}$  are the airflows into tank 6, 7 and 8. As can be seen, the airflows ( $q_{O_2,X}$ ) also has an upper limit ( $q_{O_2,X,max}$ ) due to the capacity of the compressors. Also, the dissolved oxygen concentration in the last tank should not be less than 1 mg/l.

The relationships between the airflows and  $BOD$  and  $NO$  are complex, involving the Petersen matrix in Table 2.2, the mass balances over the tanks and (2.9) and (2.11) for the oxygen transfer. Clearly, the problem is not linear.

### 3.3 Same airflow

In Equation (2.11) for the mass transfer coefficient ( $K_L a$ ) it is seen from the term  $(1 - e^{-k_2 \cdot q_{O_2}})$  that an increase in airflow is more effective at lower airflows and becomes less and less effective the higher the airflow is. By aerating as large part as possible of the activated sludge basins, the aeration should therefore be more effective since a lower total airflow will result in the same oxygen transfer as a higher airflow in a smaller part.

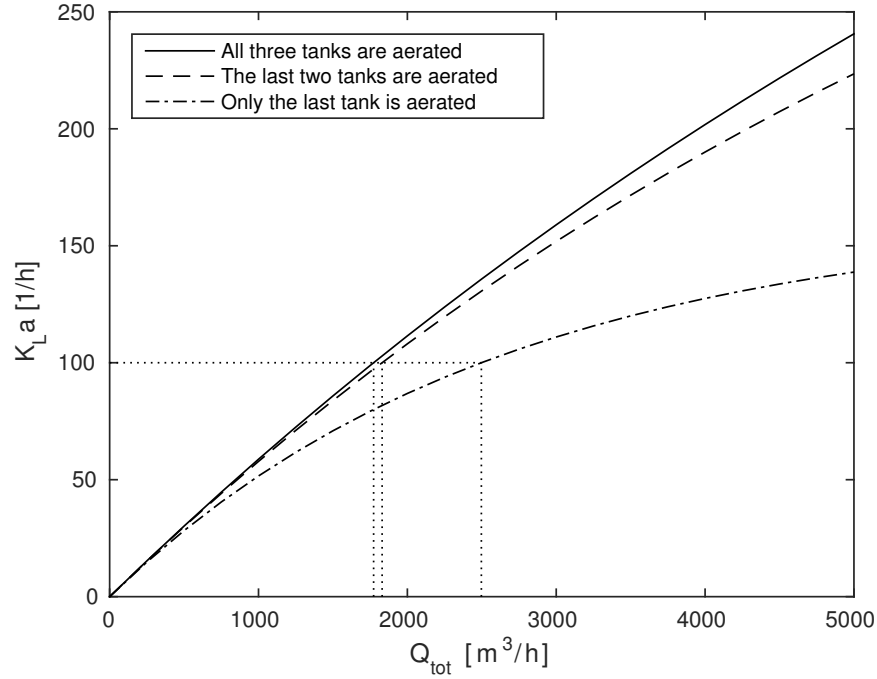


**Figure 3.1:** Mass transfer coefficient ( $K_L a$ ) depending on total airflow ( $q_{O_2, tot}$ ) for one, two and three tanks aerated.

Indeed, as seen in Figure 3.1, the same (total) mass transfer coefficient,  $K_L a$ , is achieved using less total airflow,  $q_{O_2, tot}$ , as a larger part of the activated sludge basins are aerated.

Aerating a larger part of the basins, however, results in a smaller anoxic part. This can result in a lower reduction of nitrate and nitrite,  $NO$ , since denitrification is slower at higher concentrations of  $S_O$ .

# 4

## Simulation

### 4.1 Finding the optimal airflow

To find the optimal airflow, the Matlab command *fmincon* is used. By keeping the influent concentration constant and changing the airflow, the effect on *BOD* and *NO*, i.e. nitrite and nitrate, can be studied. Since *fmincon* only finds a local minimum, a good guess of where the optimal solution is located has to be found and used as a starting point. To study how *BOD* and *NO* depend on the aeration, a grid of solutions is calculated, and the minimum of these solutions is used as starting point. The three tanks that can be aerated, are aerated in steps of a tenth of the practical upper limit. The practical upper limit is found by studying Figure 4.1. When the graph has a low slope the aeration is almost saturated. Since a higher concentration than 4 mg/l dissolved oxygen doesn't results in any significant increase of reaction rate, this is chosen as an upper limit for the grid. The resulting optimal aeration is used to compare the currently used set point control and the variations considered in this thesis.

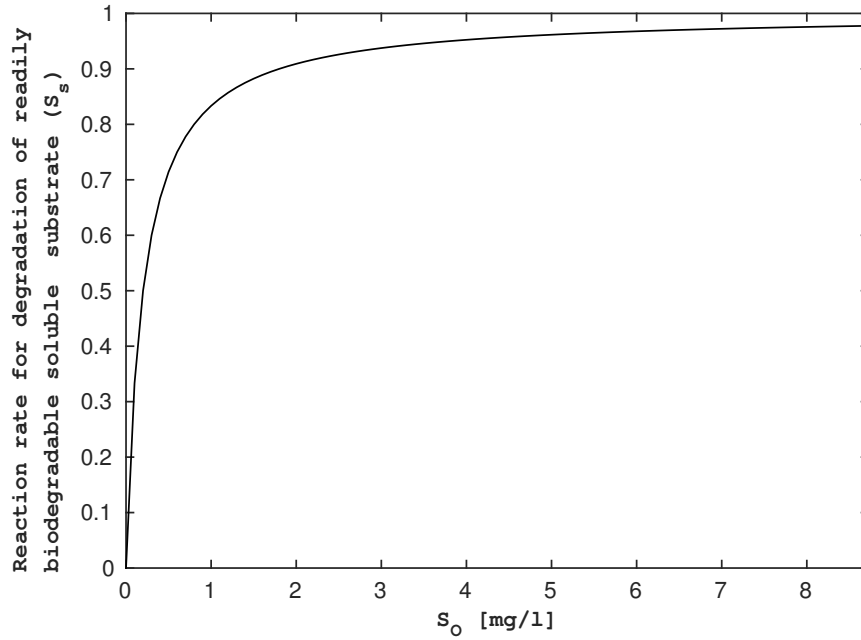


**Figure 4.1:** Reaction rate for the degradation of  $S_S$  at different concentrations of  $S_O$ .

## 4.2 The current setup

A scenario that uses a set point is simulated. This is similar to the currently used control of the aeration at the plant at Ryaverket. Simulations are run with 40% of the activated sludge basins aerated. A PI controller keeps the dissolved oxygen concentration at a level of 2 mg/l.

The controller is given a set point as input and compares that to the outgoing dissolved oxygen concentration of an activated sludge tank. The difference is used as input to a PI controller that controls the airflow of the tank. The activated sludge block is given the airflow,  $q_{O_2}$ , as an input.

### 4.2.1 Lambda tuning

Tanks 6 to 8 in the model are each subject to a step on the input that results in a change of  $S_O$  from 2.0 to 2.1 mgO<sub>2</sub>/l. The result of the step is shown in Figure 4.2 and Table 4.1.

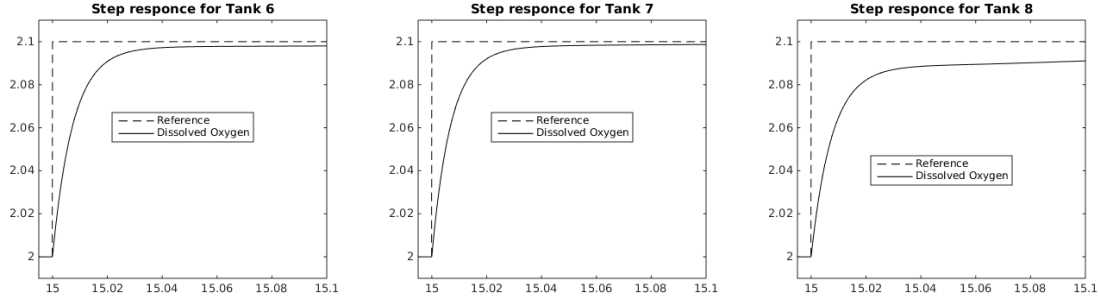


**Figure 4.2:** Oxygen concentration responses to steps in the aeration in tanks 6-8.

**Table 4.1:** First order process parameters for tanks 6-8 approximated using step responses.

	Tank 6	Tank 7	Tank 8
$K_p$	0.0029	0.0026	0.0025
$L$	0	0	0
$T$	0.0078	0.0073	0.0095

The resulting controller parameters using  $\lambda = 0.5$  are shown in Table 4.2.

**Table 4.2:** PI-controller parameters.

	Tank 6	Tank 7	Tank 8
$K_c$	680	773	788
$T_i$	0.0078	0.0073	0.0095

### 4.3 Same airflow across all tanks

This model is very similar to the current setup above, but instead of controlling each tank separately, only the last outgoing dissolved oxygen concentration is measured and all the tanks are given the same airflow. Simulations are run with both 40 % and 60 % aeration of the basins.

$$\sum_{X=6}^8 q_{O_2,X} = \sum_{X=6}^8 q_{O_2,current,X}$$

$$q_{O_2,X} = q_{O_2,Y} \quad X, Y \in [7,8] \text{ or } [6,7,8],$$

where  $q_{O_2,current,X}$  is the airflow in tank  $X$  used in simulations of the currently used setup.

#### 4.4 Minimum *BOD*, same total airflow as current

$$\begin{aligned}
& \text{minimize} && BOD \\
& \text{subject to} && \sum_{X=6}^8 q_{O_2,X} = q_{O_2,current,total} \\
& && q_{O_2,X} \leq q_{O_2,X,max} \quad X \in [6,7,8] \\
& && S_{O,8} \geq 1
\end{aligned} \tag{4.1}$$

Keeping the total airflow constant, at the same level that is currently used, and minimizing *BOD*, the optimal strategy for the distribution of aeration in the tanks can be determined.

#### 4.5 Minimum *NO*, same total airflow as current

$$\begin{aligned}
& \text{minimize} && NO \\
& \text{subject to} && \sum_{X=6}^8 q_{O_2,X} = q_{O_2,current,total} \\
& && q_{O_2,X} \leq q_{O_2,X,max} \quad X \in [6,7,8] \\
& && S_{O,8} \geq 1
\end{aligned} \tag{4.2}$$

Same approach as in the previous scenario, but now minimizing *NO* instead of *BOD* to investigate an optimal strategy to distribute the airflow over the tanks to keep *NO* at a minimum, while keeping the aeration constant.

#### 4.6 Minimum total airflow, same *BOD* as current

$$\begin{aligned}
& \text{minimize} && \sum_{X=6}^8 q_{O_2,X} \\
& \text{subject to} && BOD = BOD_{current} \\
& && q_{O_2,X} \leq q_{O_2,X,max} \quad X \in [6,7,8] \\
& && S_{O,8} \geq 1
\end{aligned} \tag{4.3}$$

Here, a constraint is added to optimize the airflow while keeping the same *BOD* as achieved by the currently used control. This result should show how to aerate the different basins in order to minimize the airflow without increasing the *BOD*-concentration in the effluent.

#### 4.7 Minimum total airflow, same $NO$ as current

$$\begin{aligned}
 &\text{minimize} && \sum_{X=6}^8 q_{O_2,X} \\
 &\text{subject to} && NO = NO_{current} \\
 & && q_{O_2,X} \leq q_{O_2,X,max} \quad X \in [6,7,8] \\
 & && S_{O,8} \geq 1
 \end{aligned} \tag{4.4}$$

Here, the constraint is changed to optimize the airflow while keeping the same  $NO$  as achieved by the currently used control. This result show how to aerate the different basins in order to minimize the airflow without increasing the  $NO$ -concentration in the effluent.

#### 4.8 Simulations using variable influent

The set points produced from the optimizations above are then simulated for a variable influent. The variations of  $BOD$  and  $NO$  over time are shown in Figures 4.3 and 4.4.

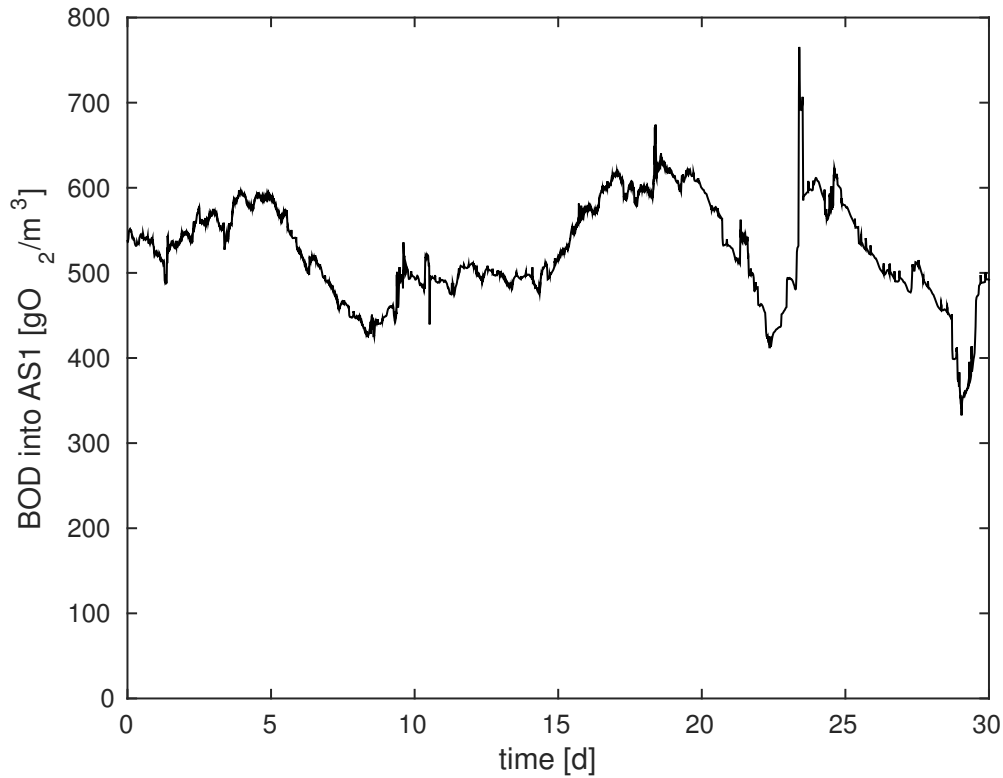


**Figure 4.3:** Concentration of  $BOD$  in the influent to the activated sludge basin.

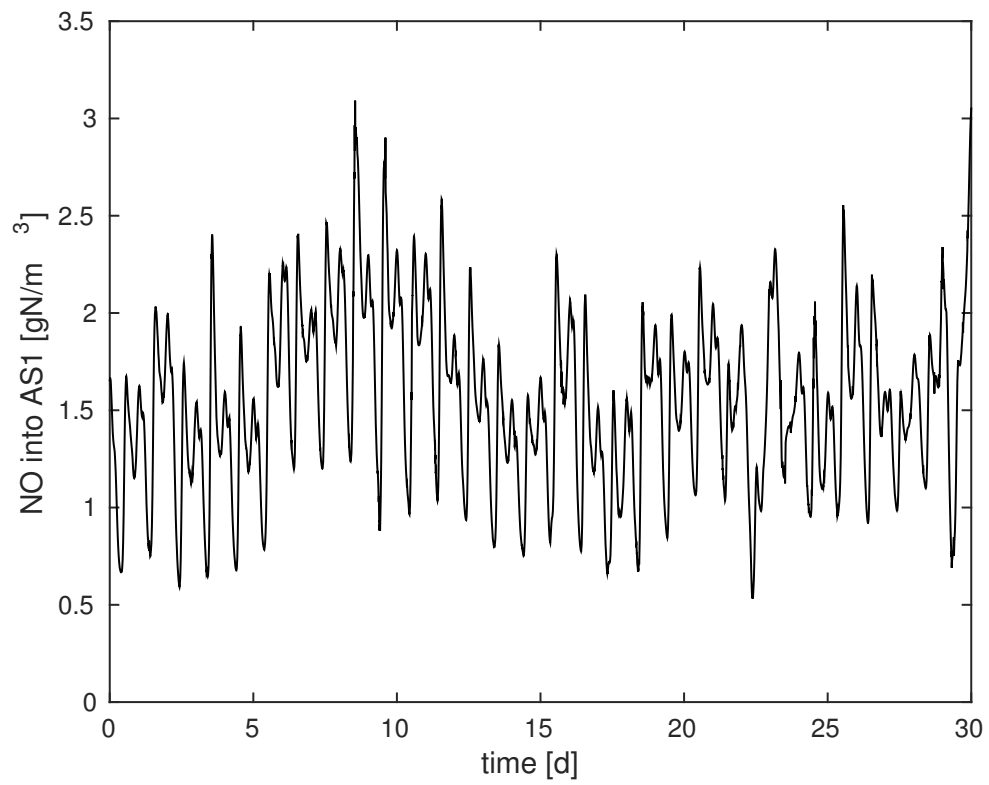


**Figure 4.4:** Concentration of *NO* in the influent to the activated sludge basin.



# 5

## Results

To keep the number of variables to a minimum in the simulations used for optimization, the influent was constant and the steady state variables of the effluent was used as results.

To investigate that the results also are "valid" for variable influent, the same set points found in the optimizations were used in simulations with variable influent.

In both cases the simulation periods were 60 days and the effluent used in the comparisons in the case with variable influent was the mean value over the last 30 days.

### 5.1 The current setup

This result is used as a benchmark for the different control strategies investigated. The results are shown in Figure 5.1 and this simulation is used as a reference point for the effectiveness of the other simulations illustrated in Figure 5.2.

### 5.2 Same airflow across all tanks

As seen by Figure 5.2, the effect of distributing the airflow evenly over 40 % of the basins compared to the current setup is very small. Keeping the same total airflow but distributing the air over 60 % has a large positive effect on the reduction of *BOD* but considerably less *NO* is removed.

### 5.3 Minimum *BOD*, same total airflow as current

This result is similar to the one with the same airflow over 60 % above. As seen in Figure 5.1, the aeration in this scenario is almost evenly distributed among the tanks. This results in a larger part of the basins with high concentrations of  $S_O$  and good *BOD* removal properties. The set points are shown in Table 5.1.

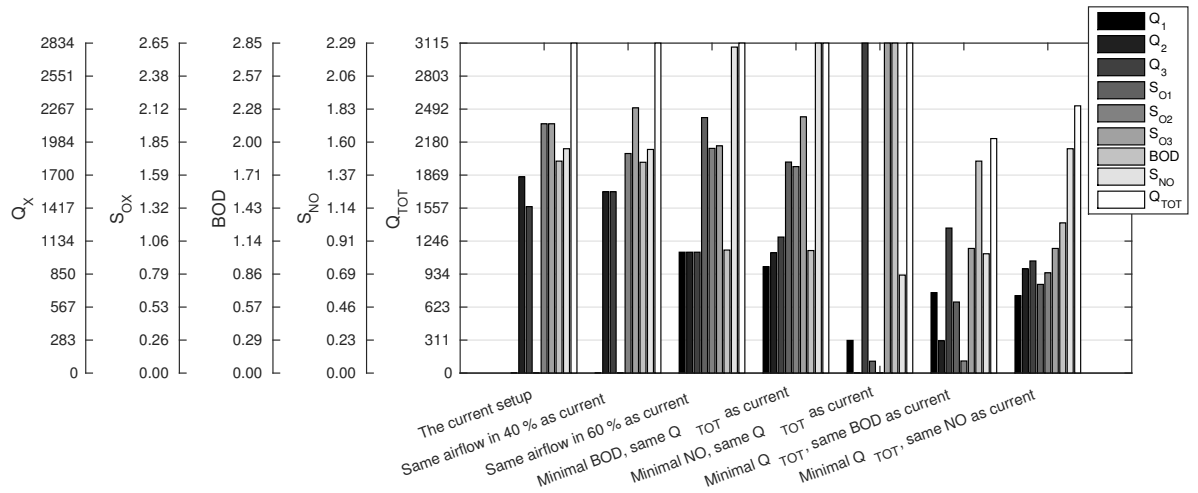


**Figure 5.1:** Results from simulation over 60 days with constant inflow variables.

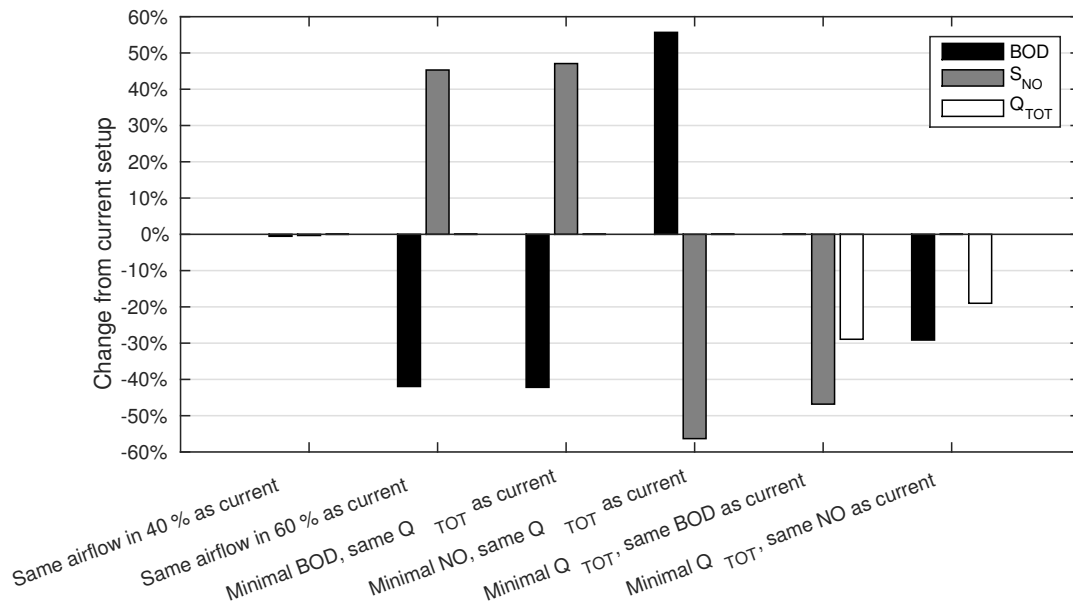


**Figure 5.2:** Change in percent from the currently used control in simulations over 60 days with constant inflow variables.

**Table 5.1**

$SP_{S_{O,6}}$	$1.69 \text{ gO}_2/\text{m}^3$
$SP_{S_{O,7}}$	$1.66 \text{ gO}_2/\text{m}^3$
$SP_{S_{O,8}}$	$2.06 \text{ gO}_2/\text{m}^3$

## 5.4 Minimum $NO$ , same total airflow as current

In this scenario more  $NO$  is reduced but much less  $BOD$  is removed, as seen in Figure 5.2. By studying Figure 5.1 and Table 5.2, it is found that nearly all air is pumped into the last tank. This is expected, since less concentration of  $S_O$  in Tanks 6 and 7 extends the anoxic zone and hence a better reduction of  $NO$  is achieved.

**Table 5.2**

$SP_{S_{O,6}}$	$0.10 \text{ gO}_2/\text{m}^3$
$SP_{S_{O,7}}$	$0.00 \text{ gO}_2/\text{m}^3$
$SP_{S_{O,8}}$	$2.65 \text{ gO}_2/\text{m}^3$

## 5.5 Minimum total airflow, same $BOD$ as current

Minimizing the total airflow and keeping  $BOD$  at the same level as in the currently used setup results in a better reduction of  $NO$  and a lower total airflow, as seen in Figure 5.2. The optimal distribution of air is controlled by the set points shown in Table 5.3.

**Table 5.3**

$SP_{S_{O,6}}$	$0.57 \text{ gO}_2/\text{m}^3$
$SP_{S_{O,7}}$	$0.10 \text{ gO}_2/\text{m}^3$
$SP_{S_{O,8}}$	$1.00 \text{ gO}_2/\text{m}^3$

In Tank 8 the lowest allowed concentration of  $S_O$  is used and that is why Tank 7 has such a low set point.

When an optimization without the lower bounds on the concentration of  $S_O$  is executed, all air is in Tank 6 and 7, as seen in Table 5.4.

**Table 5.4**

$SP_{S_{O,6}}$	$0.82 \text{ gO}_2/\text{m}^3$
$SP_{S_{O,7}}$	$0.52 \text{ gO}_2/\text{m}^3$
$SP_{S_{O,8}}$	$0.00 \text{ gO}_2/\text{m}^3$

This explains the odd composition of the set points.

## 5.6 Minimum total airflow, same *NO* as current

Keeping *NO* at the same level as the currently used setup and at the same time minimizing the total airflow results in a higher reduction of *BOD* as well as a lower total airflow (see Figure 5.2).

The resulting oxygen set points are shown in Table 5.5.

**Table 5.5**

$SP_{S_{O,6}}$	0.71 gO <sub>2</sub> /m <sup>3</sup>
$SP_{S_{O,7}}$	0.80 gO <sub>2</sub> /m <sup>3</sup>
$SP_{S_{O,8}}$	1.00 gO <sub>2</sub> /m <sup>3</sup>

## 5.7 Simulations using variable influent

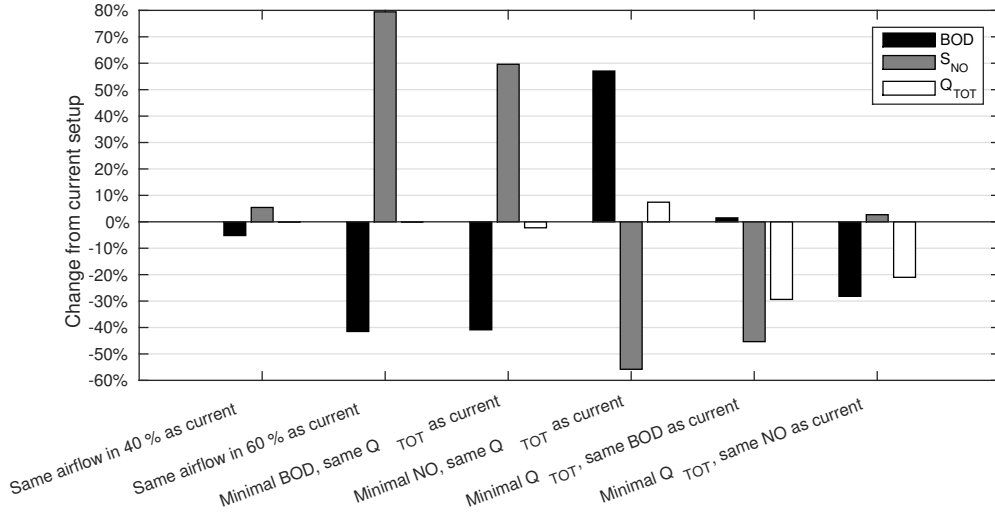


**Figure 5.3:** Change in percent from the currently used control in simulations of 60 days with variable inflow variables.

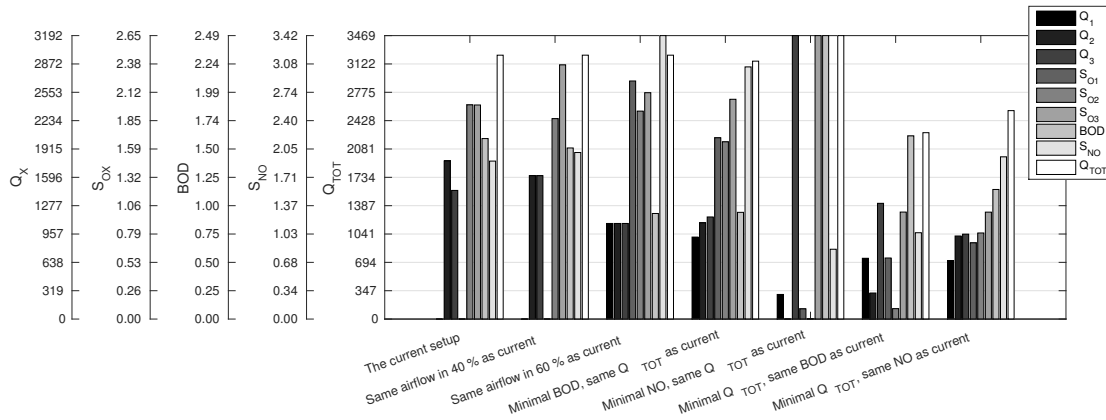


**Figure 5.4:** Results from simulation of 60 days with variable inflow variables.

Simulations are performed using variable influent and the set points for  $S_O$  from the optimizations using constant influent. As seen in Figures 5.3 and 5.4, the results are similar to the results for constant influent shown in Figures 5.2 and 5.1. There are small differences between the simulations with constant and variable influent. But the important differences remains. The results from minimizing the airflow and keeping  $BOD$  or  $NO$  constant are still an improvement of the currently used control.

More details for these results are given in Appendix A.



# 6

## Discussion

As seen in Figures 5.1 and 5.4 the best reductions of *BOD* and *NO* are achieved when a larger part is aerated with lower concentrations of  $S_O$ . In the scenarios with lowest *NO*, most air is pumped into the last tank. In the scenarios with low *BOD* the aeration is more evenly distributed.

Depending on which of the two pollutants, *BOD* or *NO*, that is more important to reduce at the moment, the set points for  $S_O$  should be adjusted accordingly. During high concentrations of *NO* in the influent the set point configuration shown in Table 5.3 should be used and when *BOD* concentrations are high the configuration shown in Table 5.5 should be used.

In general, the simulations shows that less is more. In the scenarios that reduces *BOD* without increasing *NO*, and vice versa, the total airflow is also reduced. The reason is that more of the activated sludge basins are aerated. To aerate 60 % instead of 40 % at a lower  $S_O$  concentration reduces the cost of aeration at the same time as the reduction of *BOD* and *NO* are higher.

It might not be possible to have as low set points as suggested in this report due to growth of undesired bacteria. But the simulations clearly indicates that expanding the aeration volume with only a moderate reduction of aeration can reduce costs and pollutions considerably. The cost of aeration can be lowered by as much as 30 % without increasing *BOD* or *NO* in the effluent. According to Neth [4], the annual cost of aeration is approximately 3 700 000 SEK/year which gives a potential maximum saving of over 1 000 000 SEK/year. In reality this number is most likely much smaller, but there is potential to save a significant sum each year.

Since Table 5.3 has such a low set point in Tank 7 the air may not be enough to mix the tank properly. To fully use this control strategy at site, it may be necessary to install a stirrer for the affected parts of the basins.

The accuracy of the model is as good as the parameters used. Further work should investigate also the dynamics of the plant and tune relevant parameters. The parameters

used in the model have only been tested and validated under normal operation and not at as low concentrations of  $S_O$  as suggested here.

The parts of the model that includes the settler and the trickling filters are extremely simplified. As long as the process is working in a similar state in the different scenarios the results should be good enough to evaluate the advantages and disadvantages of the different control strategies discussed here.

The control strategies in this thesis is of a constant nature, where a set of set points are used to control the aeration of the basins. Further studies that investigates the possibility to control the aeration using input from an  $NO$ -sensor should be preformed. By aerating smaller parts of the basins when the concentration of  $NO$  is high, more  $NO$  can be removed while still having a good reduction of  $BOD$  when the concentration of  $NO$  is low.



# 7

## Conclusion

By aerating a larger part of the activated sludge basins, 60 % instead of 40 %, both cost and effluent concentrations of *BOD* and *NO* are reduced. Depending on if *BOD* or *NO* is the compound that is most important to reduce, the airflow should be distributed differently between the tanks.

There is a risk of growth of unwanted bacteria if the concentration of  $S_O$  is low. Since the concentrations recommended in this thesis is considerably lower than the concentrations used today, the concentration of  $S_O$  could be lowered in small steps during a long period of time, at the same time as the quality of the effluent is closely monitored.

Strategies to reduce either *BOD* or *NO*, and at the same time lower the cost of aeration, have been found. The potential of saving money on the reduced aeration is also found to be significant.



# A

## Tables

**Table A.1:** Results from simulations with constant influent.

	$S_{O,6}$	$S_{O,7}$	$S_{O,8}$	$q_{O_2,6}$	$q_{O_2,7}$	$q_{O_2,8}$	$BOD$	$S_{NO}$	$q_{O_2,total}$
The current setup	0.00	2.00	2.00	0	1402	1012	3.78	0.56	2414
Same airflow in 40 % as current	0.00	1.55	2.22	0	1207	1207	3.78	0.55	2414
Same airflow in 60 % as current	0.77	1.16	1.56	805	805	805	2.10	0.73	2414
Minimal $BOD$ , same $q_{O_2,tot}$ as current	0.44	0.04	2.46	639	95	1681	3.54	0.38	2414
Minimal $NO$ , same $Q_{TOT}$ as current	0.10	0.00	2.65	281	0	2834	2.85	0.68	3115
Minimal $q_{O_2,tot}$ , same $BOD$ as current	0.30	0.11	1.00	540	277	916	3.78	0.34	1732
Minimal $q_{O_2,tot}$ , same $NO$ as current	0.41	0.76	1.00	624	741	716	2.51	0.56	2081

**Table A.2:** Results from variable influens simulations.

	$S_{O,6}$	$S_{O,7}$	$S_{O,8}$	$q_{O_2,6}$	$q_{O_2,7}$	$q_{O_2,8}$	$BOD$	$S_{NO}$	$q_{O_2,total}$
The current setup	0.00	2.00	2.00	0	1781	1448	1.59	1.91	3229
Same airflow in 40 % as current	0.00	1.87	2.37	0	1615	1615	1.50	2.01	3229
Same airflow in 60 % as current	2.22	1.94	2.11	1076	1076	1076	0.93	3.42	3229
Minimal $BOD$ , same $Q_{TOT}$ as current	1.69	1.66	2.05	923	1083	1150	0.94	3.04	3156
Minimal $NO$ , same $Q_{TOT}$ as current	0.10	0.00	2.65	277	0	3192	2.49	0.84	3469
Minimal $Q_{TOT}$ , same $BOD$ as current	0.57	0.10	1.00	684	293	1303	1.61	1.04	2281
Minimal $Q_{TOT}$ , same $NO$ as current	0.71	0.80	1.00	659	935	956	1.14	1.96	2551



# Bibliography

- [1] Gryaab. Avloppsvattenrening. Website, 2016. URL <http://www.gryaab.se/vad-vi-gor/avloppsvattenrening/>.
- [2] Mogens Henze. *Activated sludge models ASM1, ASM2, ASM2d and ASM3*, volume 9. IWA publishing, 2000.
- [3] Ulf Jeppsson. *Modelling Aspects of Wastewater Treatment Processes*. Lund Institute of Technology, 1996. ISBN 91-88934-00-4.
- [4] Maria Neth. *Morya 2010 - a modeling project*. Gryaab, 2011.
- [5] Torsten Wik. *On Modeling the Dynamics of Fixed Biofilm Reactors - with focus on nitrifying trickling filters*. PhD thesis, Chalmers University of Technology, 1999.
- [6] Marcus Hedegård and Torsten Wik. An online method for estimation of degradable substrate and biomass in an aerated activated sludge process. *Water research*, 45 (19):6308–6320, 2011.
- [7] J. Copp. *The COST Simulation Benchmark – Description and Simulator Manual*. COST (European Cooperation in the field of Scientific and Technical Research), Brussels, Belgium, 2001.
- [8] Jan Mattsson. Miljörapport Ryaverket 2012. *Gryaab rapport 2013:3*, 2012. URL <http://www.gryaab.se/wp-content/uploads/2016/06/Miljörapport-Ryaverket-2012.pdf>.
- [9] Simona Rossetti, Maria C Tomei, Per H Nielsen, and Valter Tandoi. “Microthrix parvicella”, a filamentous bacterium causing bulking and foaming in activated sludge systems: a review of current knowledge. *FEMS microbiology reviews*, 29(1):49–64, 2005.
- [10] Britt-Marie Wilén. Variation in dissolved oxygen concentration and its effect on the activated sludge properties studied at a full scale wastewater treatment plant. In *In the proceedings of IWA World Water Congress & Exhibition, 19-24 September 2010 in Montreal*, 2010.

- [11] Hélène Panagopoulos, Karl Johan Åström, and Tore Hägglund. The Lambda method for tuning PI controllers. Technical report, Department of Automatic Control, Lund Institute of Technology (LTH), 1997.